

Copyright iStockphoto.com/Mark Evans

The Potential of Partial IMUs for Land Vehicle Navigation

NASER EL-SHEIMY

DEPARTMENT OF GEOMATICS ENGINEERING, THE UNIVERSITY OF CALGARY

A general decline in the cost, size, and power requirements of electronics is accelerating the adoption of integrated GNSS and inertial technologies in consumer applications such as automotive and personal navigation systems. The combination also helps solve the problem of short-term GPS signal outages. Nonetheless, market-driven pressure to lower the cost of materials even further has researchers looking for ways to eliminate additional components from product designs. One possibility is to drop one or more of the relatively expensive gyroscopes from microelectromechanical system (MEMS) versions of inertial measurement units (IMUs). The adoption of other positioning data from the vehicle itself may just help make that possible.

GPS provides reliable long-term navigation information but requires a direct line of sight between the GPS receiver and GPS satellites. On the other hand, an inertial measurement unit (IMU) offers continuous autonomous navigation information, but its accuracy degrades over time due to the cumulative errors of the inertial sensors.

The integration of GPS's long-term stable accuracy with the continuous but short-term accuracy of an inertial navigation system (INS) can provide accurate and uninterrupted positioning for many difficult navigation scenarios. Land vehicle navigation is, in fact, one of the most challenging navigation modes because GPS signal quality degrades sig-

nificantly when a vehicle goes through urban canyons or forest canopies. Moreover, GPS signals — and, consequently, positioning information — can be completely lost when, for example, a vehicle goes through a tunnel or passes under a bridge.

With the development of low-cost, microelectromechanical (MEMS) inertial sensors and GPS technology, integrated INS/GPS systems are beginning to meet the growing demands of lower cost, smaller size, and seamless navigation solutions for land vehicles. Although MEMS inertial sensors are very inexpensive compared to conventional sensors, their cost (especially MEMS gyros) is still not acceptable for many low-end civilian applications, such as commer-

cial car navigation or personal location systems.

In an ideal case, three accelerometers and three gyroscopes — that is, a complete IMU — should be part of the IMU to faithfully portray the three-dimensional motions of a vehicle. However, the unremitting drive to reduce the cost to consumers of vehicle navigation systems has led to the development of simplified sensor configurations. Gyroscopes are usually more expensive than accelerometers in an IMU MEMS. For example, when purchased in bulk, a MEMS gyro chip currently costs about \$10 per axis or a total of \$30 for a three-dimensional IMU, not including other hardware, electronics, or digital signal processor, which is not acceptable for many appli-

GPS. The extended Kalman filter (EKF) is the most popular estimation technique for such integration. In the EKF, the INS errors are updated by the difference between GPS and INS solution.

Compared to the bias error, the effect of the scale factor error is relatively small; consequently, the latter errors are not included in the state vector. The KF error state vector used in aided INS toolbox is, therefore, a 15-state vector, as follows:

$$\mathbf{x} = \begin{bmatrix} \delta \mathbf{r}^n \\ \delta \mathbf{v}^n \\ \boldsymbol{\varepsilon}^n \\ \mathbf{d} \\ \mathbf{b} \end{bmatrix} \quad 1$$

where

- $\delta \mathbf{r}^n$ is position error vector of INS mechanization
- $\delta \mathbf{v}^n$ is velocity error vector of INS mechanization
- $\boldsymbol{\varepsilon}^n$ is attitude error vector of INS mechanization
- \mathbf{d} is the bias vector of gyros
- \mathbf{b} is the bias vector of accelerometers

The dynamic equations of the basic states (i.e. $\delta \mathbf{r}^n$, $\delta \mathbf{v}^n$ and $\boldsymbol{\varepsilon}^n$) are obtained by linearizing the INS mechanization equations. For inertial sensor biases error models, they are represented using stochastic processes. (See the publication by S. Nassar in Additional Resources for more details about various INS stochastic error models.) The toolbox uses the most commonly model for inertial sensor biases, a first-order Gauss-Markov model.

The corresponding spectral density matrix Q of the state noises is set as:

$$Q = \begin{bmatrix} q_{position} \cdot \mathbf{I}_{3 \times 3} & 0 & 0 & 0 & 0 \\ 0 & q_{velocity} \cdot \mathbf{I}_{3 \times 3} & 0 & 0 & 0 \\ 0 & 0 & q_{attitude} \cdot \mathbf{I}_{3 \times 3} & 0 & 0 \\ 0 & 0 & 0 & q_{gyro} \cdot \mathbf{I}_{3 \times 3} & 0 \\ 0 & 0 & 0 & 0 & q_{accel} \cdot \mathbf{I}_{3 \times 3} \end{bmatrix} \quad 2$$

GPS position and velocity are used as the KF update measurements in the IMU/GPS integration filter. However, in the research described in this article, GPS velocities are not used as updates because most of the newly developed, low-cost GPS chips — which will be chosen by most users for vehicle navigation applications in the future — will not have velocity output.

Therefore, the measurements vector for the KF will be the position difference between the MEMS IMU (derived from the mechanization equations) and GPS positions \mathbf{r}_{GPS}^n , that is,

$$\mathbf{z} = \mathbf{r}_{MEMS}^n - \mathbf{r}_{GPS}^n \quad 3$$

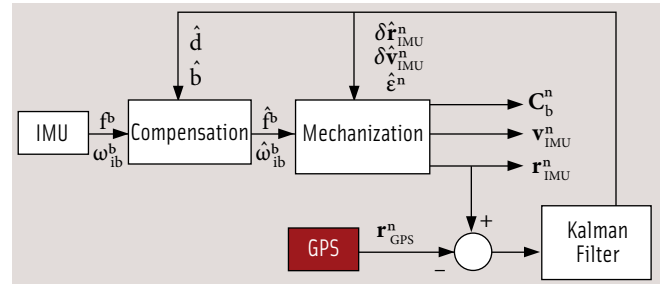


FIGURE 2 Structure of the KF for IMU/GPS integration

Figure 2 presents a block diagram of the developed navigation algorithm in which the ^ symbol means estimated or compensated quantities. The estimated gyros and accelerometers biases are fed back, as compensation, to the IMU raw measurements every time it is updated.

Vehicle Dynamic Information

The non-holonomic constraint (NHC) is applied to further improve the navigation performance. Here, NHC refers to the fact that, unless the vehicle jumps off the ground or slides on the ground, the velocity of the vehicle in the plane perpendicular to the forward direction is almost zero. This constraint can be regarded as velocity update (zero update) along the cross-track and vertical axis of the vehicle:

$$\left. \begin{aligned} v_y^b &\approx 0 \\ v_z^b &\approx 0 \end{aligned} \right\} \quad 4$$

where

- b = body frame
- y = sideways component of the velocity
- z = vertical component of the velocity

As evident from Equation 4, the velocity has to be converted into the vehicle frame to apply these NHC. Consequently, the alignment of the inertial system with the vehicle body is of prime importance when NHCs are applied. The computed velocity in the body frame can be expressed as:

$$\underline{v}^b = \hat{C}_n^b \cdot \underline{v}^n \quad 5$$

where n is the navigation frame and \hat{C}_n^b is the rotation matrix from the navigation frame to the body frame.

Considering only the first order error terms, the corresponding error equation is

$$\delta \underline{v}^b \approx C_n^b \delta \underline{v}^n - C_n^b (\underline{v}^n \times) \boldsymbol{\varepsilon}^n \quad 6$$

where

$$\delta \underline{v}^b = \begin{bmatrix} \delta v_x^b \\ \delta v_y^b \\ \delta v_z^b \end{bmatrix}$$

- $\delta \underline{v}^n$ = residual errors in the velocity vector
- $\boldsymbol{\varepsilon}^n$ = residual errors in the direction cosine matrix used to rotate the navigation frame to the body frame.

The measurement equation can be constructed from the second and third rows of Equation 6 as

$$\underline{z}_k = \begin{bmatrix} \delta v_y^b \\ \delta v_z^b \end{bmatrix} \quad 7$$

and

$$H_k = \begin{pmatrix} 0 & 0 & 0 & C_{12} & C_{22} & C_{32} & -v_D C_{22} + v_E C_{32} & v_D C_{12} - v_N C_{32} & -v_E C_{12} + v_N C_{22} \\ 0 & 0 & 0 & C_{13} & C_{23} & C_{33} & -v_D C_{23} + v_E C_{33} & v_D C_{13} - v_N C_{33} & -v_E C_{13} + v_N C_{23} \end{pmatrix} \quad 8$$

where the first three columns of the H matrix corresponds to the position errors in the state vector, the second set of three columns corresponds to the velocity errors, and the last set corresponds to the angular displacements with the C_{xx} terms computed from Equation 9:

$$C_b^n = \begin{bmatrix} C_{11} & C_{12} & C_{13} \\ C_{21} & C_{22} & C_{23} \\ C_{31} & C_{32} & C_{33} \end{bmatrix} \quad 9$$

The estimated errors are then fed back to correct the INS mechanization solution as shown in **Figure 3**.

Vehicle Frame Measurements

Complementing the NHC, the odometer (or anti-lock braking system “ABS”) signal can be regarded as the velocity update along the forward (along-track) direction, as follows:

$$v_x^b \approx v_{odom} \quad 10$$

where

v_x^b is velocity projection in the body frame along forward direction and

v_{odom} is the derived speed from the odometer signals.

To satisfy the condition as closely as possible, wheel sensors need to be

installed on rear wheels if the front wheels are used for steering. Then, the relationship between the velocity of the vehicle at the center of the IMU, V_{IMU}^n , and that at the wheel, V_{odom}^v can be expressed as

$$V_{odom}^v = C_b^v C_n^b V_{IMU}^n + C_b^v \Omega_{nb}^b \lambda_{odom}^b \quad 11$$

where λ_{odom}^b is the lever-arm vector of the wheel sensor in the b-frame. Equation 11 will be disturbed if significant slips exist. Therefore, the NHC and the odometer signal comprise a com-

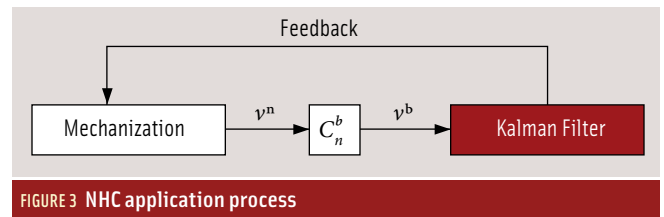


FIGURE 3 NHC application process

plete three-dimensional velocity update in the vehicle (body) frame:

$$v^b \approx \begin{bmatrix} v_{odom} \\ 0 \\ 0 \end{bmatrix} \quad 12$$

Note that these two updates should be applied at the contact point of the wheel where the odometer sensor was installed. Lever-arm conversion between this point and the reference point is necessary before applying the updates.

We also need to consider possible misalignment between the IMU frame and the vehicle frame, where the velocity constraint applies. In the same fashion as the other update measurements, these two components of aiding information have errors.

Vehicle sliding and bumping will violate the NHC and affect the accuracy of the odometer. Therefore, an appropriate error level, i.e., the covariance matrix of the update measurements, should be assigned and tuned to achieve the optimal effect.

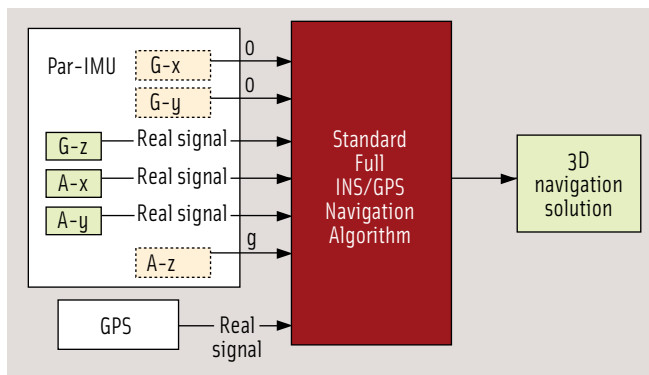


FIGURE 4 Principle of the ParIMU processing algorithm based on pseudo sensors

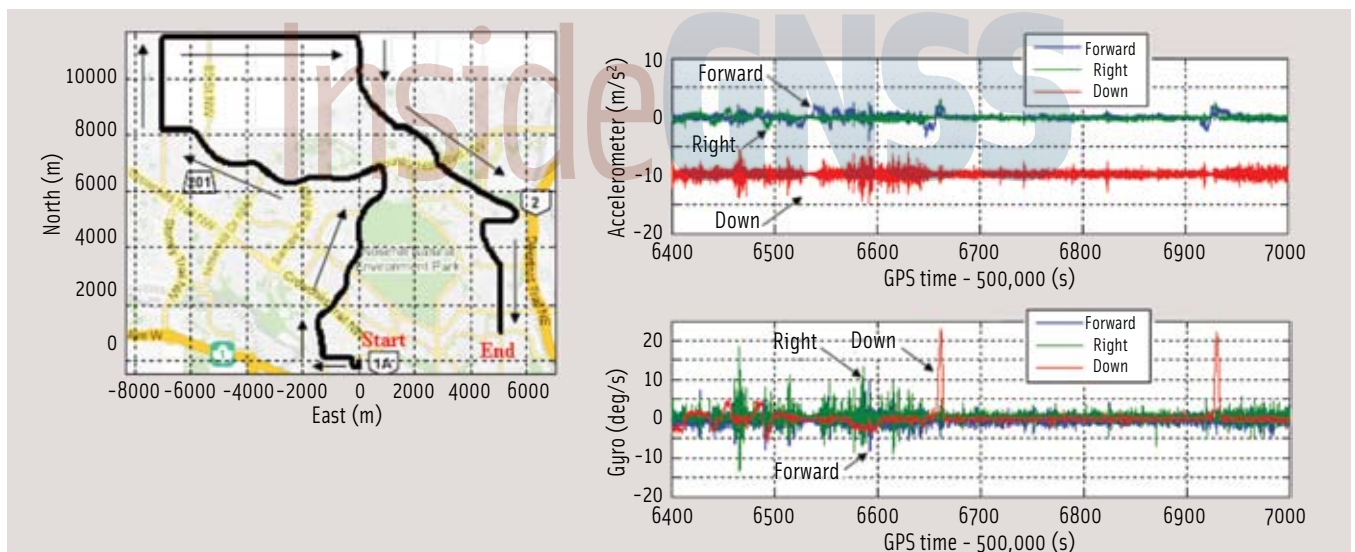


FIGURE 5 Field trial trajectory and MEMS-based inertial sensor signals in a typical land vehicle environment

Partial IMUs

The most popular partial IMU configuration for land vehicles consists of one heading gyro (Gz) plus two horizontal accelerometers (Ax and Ay), which we denote as 1G2A. This design is based on the fact that the removed sensors provide minimal navigation information for land vehicles. For example, the vertical accelerometer (Az) mainly outputs constant gravity plus vehicle bumps, while the roll and pitch gyros (Gx and Gy) are mainly sensing the angular bumping of the vehicle. Besides, land vehicle navigation normally concentrates on the horizontal location rather than the vertical height.

Considering that MEMS gyros are the most expensive IMU component, the 1G2A configuration can reduce the sensor cost by 50 to 65 percent. Another possible partial IMU configuration is 1G3A, which includes one vertical gyro and the full triad of accelerometers. In the following section, we will show the gain of adding the extra accelerometer.

Conventional methods to process the ParIMU signal develop a specific simplified INS mechanization and Kalman filter. The other way to process the ParIMU data without having to change the navigation algorithms introduced in the previous section is to introduce pseudo sensors (or pseudo signals) for the missing sensors. This then allows us to process the ParIMU data using standard GPS/INS navigation algorithms, which are designed to process the full IMU signals. Concretely, we replace the omitted sensor signals with pseudo signals, which are constant zero for the horizontal gyros (i.e., Gx and Gy) and constant local gravity for the vertical accelerometer. We then feed these into the standard GPS/INS algorithm together with the real sensor signals (as shown in Figure 4).

To be used in the KF algorithm, a pseudo signal has to satisfy the KF Gaussian white noise requirements. This can be accomplished by calculating the spectral density Q, described in Equation 2, of the pseudo signal error by using the standard deviation (STD) of the signal and the bandwidth (BW) of the

IMU. For example, this can be calculated for the accelerometers q_{accel} as follows:

$$\sqrt{q_{\text{accel}}} = \frac{\text{STD}_{\text{accel}}}{\sqrt{\text{BW}_{\text{IMU}}}} \quad 13$$

Figure 5 shows the trajectory and the signals from the accelerometers and gyros that are typical for land vehicles. This figure reveals some important facts that support the idea of using partial IMUs. First, because land vehicles mainly run on flat roads, the output of the vertical (z-axis) accelerometer is primarily composed of the local gravity plus the addition of road vibrations or undulations. As a result, because it seems to carry less navigation information, the z-axis accelerometer can be excluded to save cost and size of the system.

The second conclusion that can be made about the two MEMS horizontal gyros is that their signals can be regarded as zero mean white noise. Hence, both horizontal gyros contribute very little important navigation information and, consequently, these sensors may be excluded from the full IMU configuration to save cost and reduce the size of the navigation system.

For the vertical accelerometer signal, the values for the $\text{STD}_{\text{accel}}$ and BW_{IMU} are 0.45 m/s^2 and 50.0 Hz , respectively. Substituting these values in Equation 13, can be obtained as

$$\sqrt{q_{\text{accel}}} = \frac{\text{STD}_{\text{accel}}}{\sqrt{\text{BW}_{\text{IMU}}}} = \frac{0.45 \text{ m/s}^2}{\sqrt{50.0 \text{ Hz}}} = 0.064 \text{ m/s} / \sqrt{s} \quad 14$$

This value can be then be used to set the relevant KF parameter, i.e., the component in the spectral density matrix (Q, Equation 2) that corresponds to the noise of the pseudo signal. Similarly, the spectral densities of the two pseudo gyros (q_{gyro}) can be obtained using a similar formula that considers the gyro signals.

A minor issue of this processing method is that the actual error of the pseudo signals may not be mainly white noise. In this case, other error components may mislead the KF and cause divergence of the solution especially during GPS signal outage periods. However, in the worst case scenario, the pseudo signal parameters in the KF — that is, their corresponding components in the spectral density matrix — can be set large enough so that these pseudo signals will not take effect in the navigation algorithm.

Results and Analysis

To demonstrate the performance of the partial IMUs, the proposed pseudo signal, and the processing method, two ParIMU configurations, namely, 1G2A and 1G3A, will be compared to the full IMU results through a field testing of a land vehicle. The test includes the MEMS IMU/GPS navigation system developed by the MMSS group at the University of Calgary, a self-developed MEMS IMU, and a high-precision GPS receiver integrated with a navigation-grade IMU.

A differential GPS/navigation-grade IMU configuration provided the reference solution (i.e., true values) for the MEMS

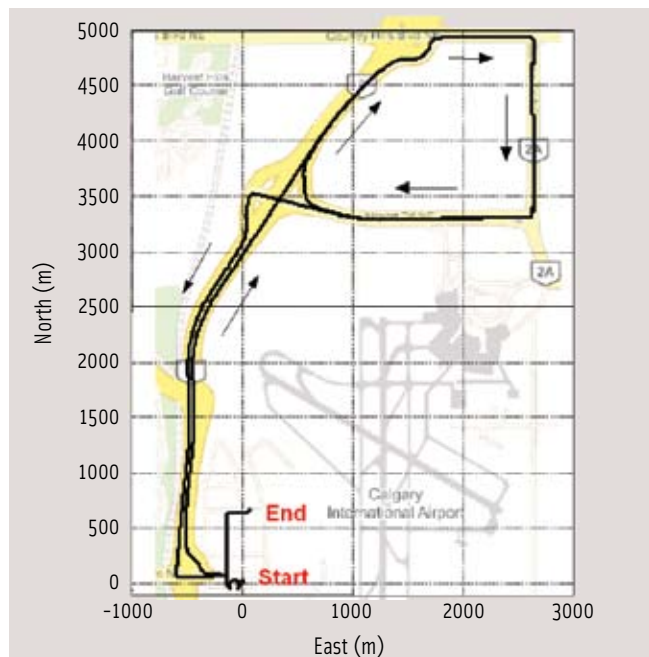


FIGURE 6 Trajectory of the field test

system analysis. Figure 6 shows the test trajectory. The full IMU and partial IMU configurations are processed incorporating single-point GPS (SPGPS) position data. Short-term GPS signal outages (10 and 30 seconds) were simulated to evaluate the performance of the various IMU configurations in stand-alone mode. The analysis of the results also address the three questions defined at the outset of this article:

Is the degradation in accuracy with a ParIMU worth considering given the reduction of cost? Two different ways were used to answer this question. The first approach compared the position and attitude drifts of the two ParIMU configurations during GPS signal outages with drift performance of the full IMU (the benchmark for the analysis). The second method compared the percentage of the drift to the traveled distance (which is much easier to understand, especially for land vehicle navigation applications).

Can we use the same full-IMU processing techniques with partial IMUs? The answer to this question comes from a straightforward comparison of the results of partial IMU configurations and the full (i.e., three-axis) IMU while GPS signals were available.

Can we improve the accuracy of the partial IMU using other aiding sources during the absence of GPS signals? For this question, we processed GPS/inertial data while applying NHC and odometer updates.

Figure 7 shows the mean positional errors (along-track, cross-track, and 2D) obtained during two GPS signal outage periods (10 and 30 seconds). Figure 8 displays the corresponding results when the NHCs were applied. Both figures confirm that the performance of both ParIMU configurations (1G2A and 1G3A) is almost the same. Therefore, the next analysis of the potential of partial IMUs concentrates only on the 1G2A configuration.

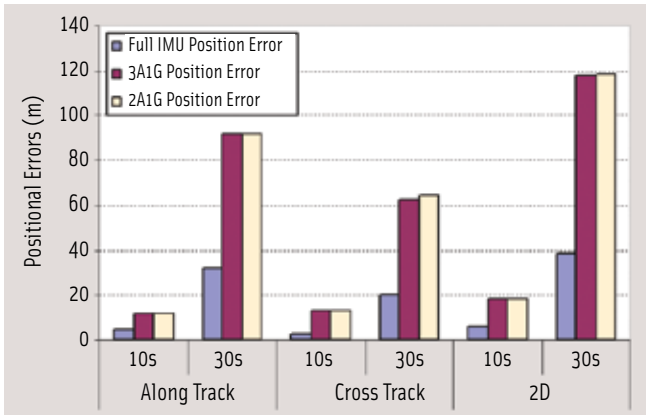


FIGURE 7 Full IMU, 1G2A and 1G3A position errors during GPS signal outages (without applying NHC)

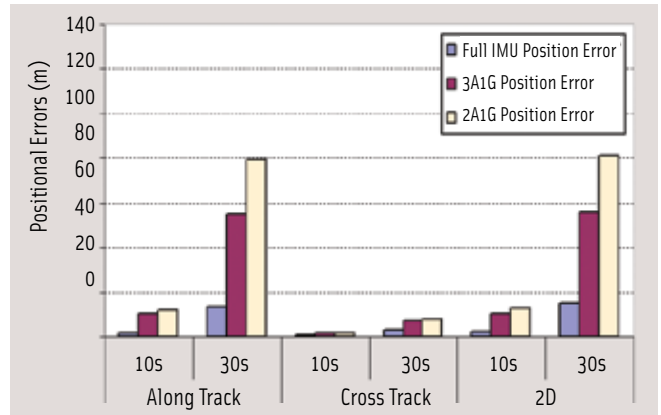


FIGURE 8 Full IMU, 1G2A and 1G3A position errors during GPS signal outages (applying NHC)

We should emphasize here, however, that the successful implementation of any of the partial IMU configurations, 3A1G or 2HA1G, assumes that the two horizontal accelerometers are “horizontal,” that is, leveled when NHC is not applied. When applying NHCs, the system should be leveled within an angle of +/- 5 degrees.

Any tilting beyond these limits will substantially worsen the obtained accuracy. For more details on the degradation of navigation accuracy due to poorly aligned inertial sensors, readers may consult the paper by Z. Syed et alia cited in Additional Resources.

Finally, the summary of the different MEMS sensor configurations (full IMU, 1G2A, and 1G3A) performance (as a percent of position errors over traveled distance) during the various kinematic

GPS outage periods (10, 30, and 60 seconds) is given in Table 1 and Table 2, for the two cases: without and with applying NHC, respectively. Table 1 and Table 2 reflect the remarkable effect of applying NHC on the cross-track position errors where the ($\Delta P/D$) percentages are in the levels of 1, 1.3, and 3 percent for the 10-, 30- and 60-second GPS outage periods, respectively.

The results of the full IMU and 1G2A ParIMU integrated with SPGPS are shown in Figure 9 A and B. The upper subplot in each figure shows the position error during eight 30-second simulated GPS signal outages, while the lower subplots show the attitude errors. The figure clearly indicates that for the full IMU large position drifts occur during GPS signal blockages, which is typical for MEMS systems. The azimuth has some

drift error, which is caused by the lack of kinematics and the GPS signal loss.

Compared to the full IMU, the 1G2A ParIMU configuration results in Figure 9B shows that the position drifts much faster after losing GPS; the roll and pitch errors get much noisier and have some small linear drifts; and the heading drift becomes larger.

These degradations can be explained by the omitted inertial sensors. The missing roll and pitch gyros make the system unable to track the quick tilt-angle changes. The tilt error then projects the incorrect projection of the gravity in the horizontal plane, which then generates velocity and position drifts once the GPS signal is lost. Because the three axis attitude angles are coupled, degraded roll and pitch also affect the azimuth estimation.

		Along Track			Cross Track			2D		
GPS Outage Interval		10s	30s	60s	10s	30s	60s	10s	30s	60s
Used IMU Type										
Full IMU	(dP/D) %	2.47	5.44	10.02	1.55	3.45	10.33	3.93	7.28	16.97
1G3A	(dP/D) %	6.53	15.61	24.46	7.00	10.66	28.16	12.5	22.7	41.1
1G2A	(dP/D) %	6.49	15.55	24.42	7.07	10.94	28.07	12.6	22.9	41.0

TABLE 1. Full IMU, 1G2A and 1G3A position errors/traveled distance percentage during kinematic GPS signal outages (without applying NHC)

		Along Track			Cross Track			2D		
GPS Outage Interval		10s	30s	60s	10s	30s	60s	10s	30s	60s
Used IMU Type										
Full IMU	(dP/D) %	0.96	2.33	4.08	0.64	0.60	1.35	1.68	3.01	4.40
1G3A	(dP/D) %	5.65	9.33	10.36	1.07	1.18	3.05	7.2	9.5	11.4
1G2A	(dP/D) %	6.66	9.86	13.56	1.00	1.34	2.87	7.8	10.7	13.7

TABLE 2. Full IMU, 1G2A and 1G3A position errors/traveled distance percentage during kinematic GPS outages (applying NHC)

Figure 10 A and B show the corresponding results when applying the NHC. As expected for the full IMU, NHC helps to suppress the position drift during GPS signal outages and also constrains the azimuth drift significantly. These improvements can also be observed for the 1G2A ParIMU configuration results. But the position drifts of the 1G2A ParIMU configuration are still larger than those of the full IMU, and the roll and pitch errors are still noisy.

Note that the slight linear drift of pitch in Figure 9-B disappears in Figure 10-B, which indicates the observability of NHC to the pitch angle. Some small position biases (several meters) can be noticed, which are due to the use of SPGPS. For the ParIMU with NHC, the performance is fairly acceptable for some land vehicle navigation applications.

The odometer update is then applied together with the NHC. **Figure 11** shows the RMS error performance of 1G2A ParIMU and full IMU configurations with NHC and odometer updates during 30-second GPS signal outages. Figure 11-A clearly shows that the position drifts during GPS gaps are further reduced.

The results can be summarized as follows:

1. When a GPS update is available, the position error is dominated by the GPS component, and both the Full IMU and ParIMU have the same level of position error; but the attitude of ParIMU is much worse than the full IMU.
2. When the GPS signals are blocked, the position drift of the ParIMU is much larger than the full IMU.
3. NHC and odometer can suppress the position drift and the azimuth error of the ParIMU significantly, similar to the full IMU.
4. The more aiding information used, the less difference between full IMU and ParIMU, since the system solution in these cases counts on the IMU less.

However, compared to the full IMU, the 1G2A ParIMU configuration has obvious degradations, but the navigation accuracy is still acceptable for some commercial applications that consider

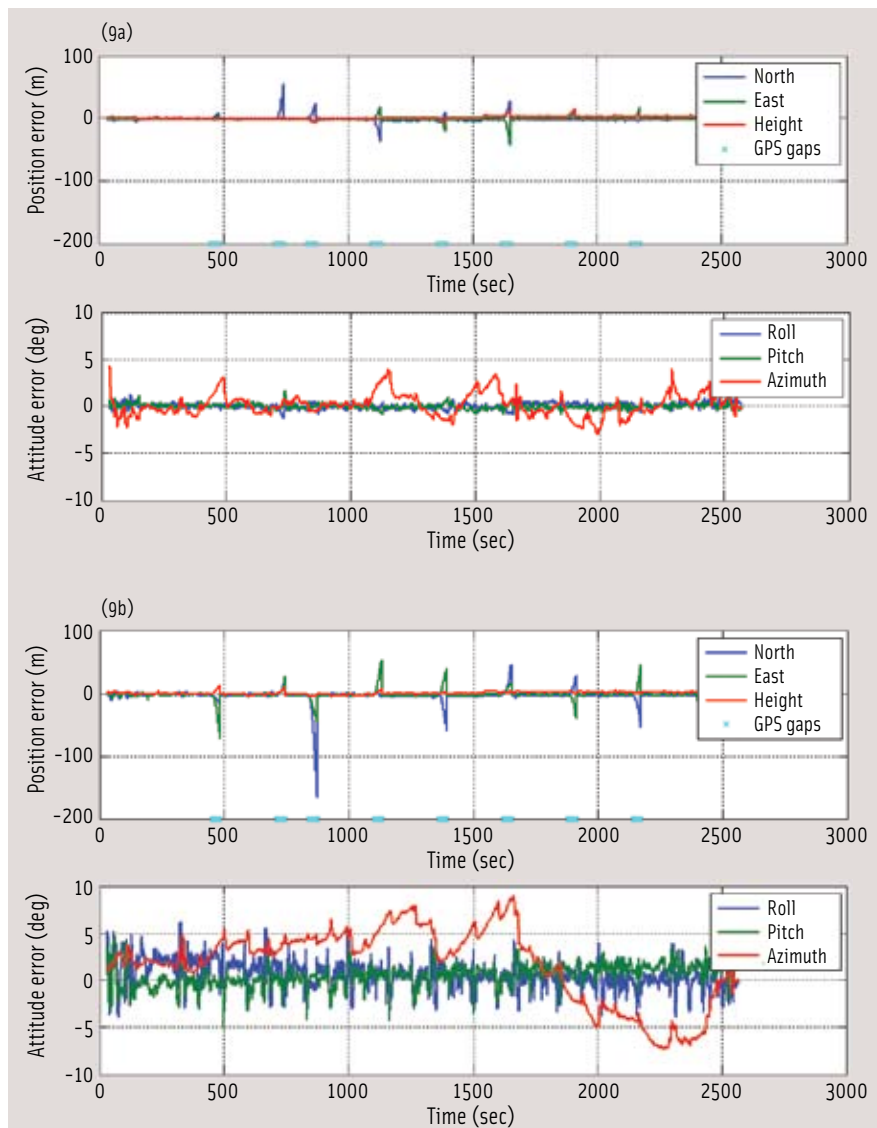


FIGURE 9 a) Navigation errors of the full IMU/SPGPS during GPS signal outages b) Navigation errors of the ParIMU/SPGPS during GPS signal outages

cost as the main concern and can afford some performance degradation.

Summary and Conclusions

This research attempted to meet the two challenges of the current MEMS Inertial/GPS navigation systems, i.e. reducing the cost and improving the performance, by introducing a partial IMU (ParIMU) configuration, and applying two different methods to improve the navigation performance of partial IMUs through the use of additional information (NHC and odometer).

Testing of a ParIMU configuration consisting of one vertical gyro and two horizontal accelerometers (1G2A) can reduce the inertial sensor cost by 50 to

65 percent, while maintaining an acceptable navigation performance with some external aiding (NHC and odometer update) which proved to be a very promising design for land-vehicle navigation applications.

Manufacturers

The toolbox software used to analyze the results of the research described in this article is the Aided Inertial Navigation System Toolbox (AINS) for MatLab Software developed by the **Mobile Multi-Sensor Systems (MMSS) Research Group** at the University of Calgary. An OEM 4 receiver from **NovAtel, Inc.**, Calgary, Alberta, Canada, coupled with the CIMU navigation-grade IMU from

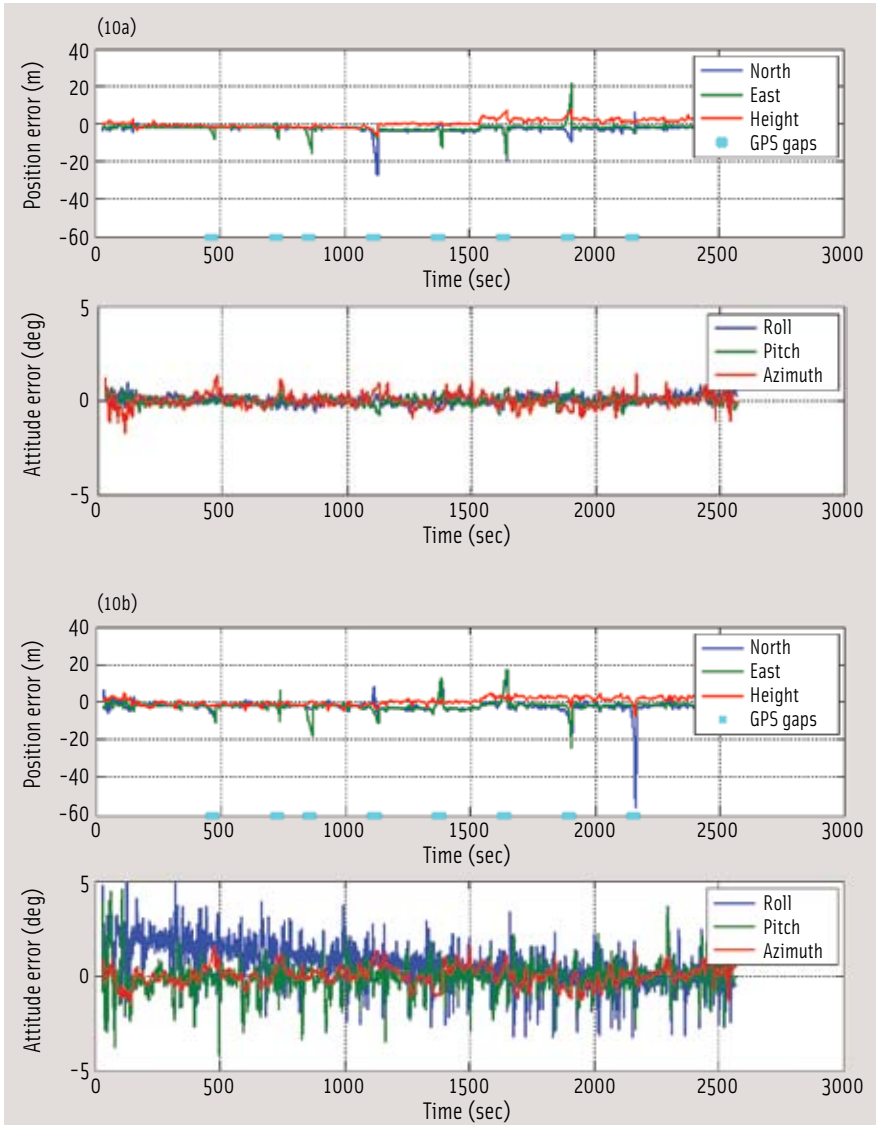


FIGURE 10 a) Navigation errors of the full IMU/SPGPS during GPS signal outages (with NHC)
 b) Navigation errors of the ParIMU/SPGPS during GPS signal outages (with NHC)

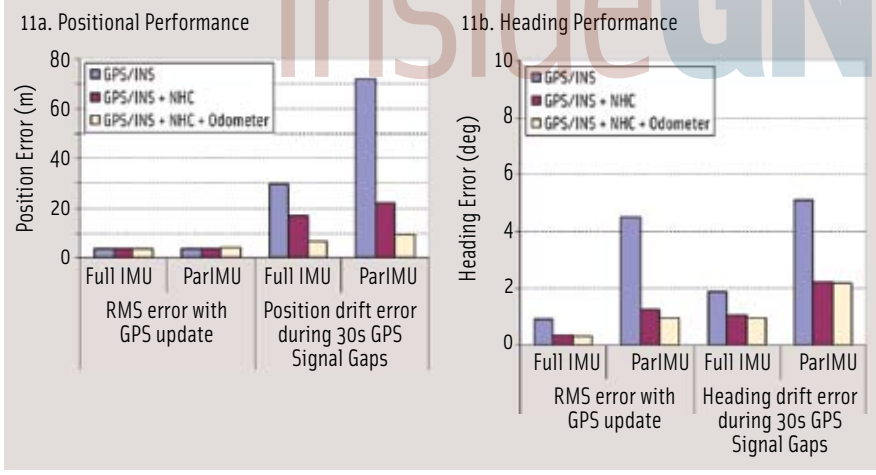


FIGURE 11 Performance of 1G2A ParIMU and full IMU Configurations with NHC and Odometer Updates

Honeywell Inc. was used as the benchmark “truth” system for the tests. The full and partial IMUs developed by the MMSS group incorporated ADXL105 accelerometers and ADXRS150 gyroscopes from Analog Devices Inc. (ADI), Norwood, Massachusetts, USA.

Acknowledgments

This study was funded by research grants from Natural Science and Engineering Research Council of Canada (NSERC) and Geomatics for Informed Decisions (GEOIDE), Network Centers of Excellence (NCE) awarded to Dr. Naser El-Sheimy. The author would like to thank (1) his former Ph.D. student, Dr. Eun Shin as a co-author — along with the author of this article — of the AINS software used in this research, (2) his current and former research team members, Dr. Kai-Wei Chiang, Dr. Dongqing Gu, Dr. Sameh Nassar, Bruce Wright, Chris Goodall, and Zainab Syed, for their help in collecting the datasets used in this article, and (3) his former post-doctorate fellow, Dr. Xiaoji Niu, and his current research engineer, Bruce Wright, for their help in developing the ADI MEMS IMU used in the dataset described in this article.

Additional Resources

Analog Devices Inc., “Datasheet of High Accuracy $\pm 1\text{ g}$ to $\pm 5\text{ g}$ Single Axis iMEMS Accelerometer with Analog Input: ADXL105,” Norwood, Massachusetts, USA, 1999

Analog Devices Inc., “Analog Devices Introduces World’s First Integrated Gyroscope,” news releases, Norwood, Massachusetts, USA, October 01, 2002.

Analog Devices Inc. (2003). Datasheet of $\pm 150^\circ/\text{s}$ Single Chip Yaw Rate Gyro with Signal Conditioning: ADXRS150,” Norwood, Massachusetts, USA, 2003

Brandt, A., and J. F. Gardner, “Constrained Navigation Algorithms for Strapdown Inertial Navigation Systems with Reduced Set of Sensors,” *Proceedings of the American Control Conference*, Philadelphia, Pennsylvania, USA, V.3, pp.1848-1852, June 24–26, 1998

Brown, R. G. and P. Y. C. Hwang, *Introduction to Random Signals and Applied Kalman Filtering*, John Wiley & Sons Inc., 1997

Dissanayake, G., and S. Sukkarieh, E. Nebot, and H. Durrant-Whyte, “The Aiding of a Low Cost, Strapdown Inertial Unit Using Modelling XConstraints in Land Vehicle Applications,” *IEEE Transactions on Robotics and Automation*, 17(5), 731–747, 2001

El-Sheimy, N., and X. Niu, "The Development of Low-Cost MEMS-Based IMU for Land Vehicle Navigation Applications," The GEOIDE 6th Annual Meeting, Gatineau, QC, Canada, May 30–June 1, 2004

El-Sheimy, N., and E-H. Shin and X. Niu, "Kalman Filter Face-Off: Extended Versus Unscented Kalman Filters for Integrated GPS and MEMS-Based Inertial Systems," *Inside GNSS*, Vol. 1 No. 2, pp 48–54, March 2006

El-Sheimy, N., and X. Niu, "The Promise of MEMS to the Navigation Community," *Inside GNSS*, Vol. 2, No. 2, pp 26–56, pp. 46–56, March/April 2007

Gelb, A., *Applied Optimal Estimation*, The M.I.T. Press, Massachusetts Institute of Technology, Cambridge, Massachusetts, USA, 1974

Mayhew D. M. (1999). "Multi-rate Sensor Fusion for GPS Navigation Using Kalman Filtering" M.Sc. thesis, Department of Electrical and Computer Engineering, Faculty of the Virginia Polytechnic Institute and State University, Blacksburg, Virginia, USA

Nassar, S., "Improving the Inertial Navigation System (INS) Error Model for INS and INS/DGPS Applications," Ph.D. thesis, Department of Geomatics Engineering, University of Calgary, Calgary, Alberta, Canada, UCGE Report No. 20183, 2003

Peng, Y.K, and M.F. Golnaraghi, "A Vector-Based Gyro-Free Inertial Navigation System by Integrating Existing Accelerometer Network in a Passenger Vehicle," *Proceedings of IEEE Position Location and Navigation Symposium (PLANS 2004)*, pp. 234–242, Monterey, California, USA, April 26–29, 2004,

Phuyal, B., "An Experiment for a 2-D and 3-D GPS/INS Configuration for Land Vehicle Applications, *Proceedings of the IEEE Position Location and Navigation Symposium (PLANS 2004)*, pp.148–152m, Monterey, CA, April 26–29, 2004

Schwarz, K. P., and S. Nassar, "A Simple Algorithm for Bridging DGPS Outages by INS Bias Modeling" *Proceedings of the 3rd International Symposium on Mobile Mapping Technology (MMT 2001)*, Cairo, Egypt, January 3–5, 2001

Shin, E. H., and N. El-Sheimy, "Aided Inertial Navigation System (AIN-STM) Toolbox for MatLab™ Software, INS/GPS Integration Software, Mobile Multi-Sensor Systems (MMSS) Research Group, the University of Calgary, Alberta, Canada, 2004 <http://www.uti.ca/industry/technology_view.asp?TechnologyID=48>

Shin, E. H., "Estimation Techniques for Low-Cost Inertial Navigation," Ph.D. Thesis, MMSS Research Group, Department of Geomatics Engineering, University of Calgary, UCGE Report No. 20219, Calgary, Alberta, Canada, 2005

Sukkarieh, S., "Low Cost, High Integrity, Aided Inertial Navigation Systems for Autonomous Land Vehicles," Ph.D. thesis, Australian Centre for Field Robotics, Department of Mechanical and Mechatronic Engineering, The University of Sydney, Sydney, Australia, 2000

Syed, Z., and P. Aggarwal, X. Niu, and N. El-Sheimy, "Accuracy Degradation of MEMS Integrated Navigation Systems Due to Poorly Aligned Inertial Sensors," ION National Technical Meeting 2007, , San Diego, California, USA, January 22–24, 2007

Author



Naser El-Sheimy is the head of the Department of Geomatics Engineering and leader of the Mobile Multi-sensor Research Group at the University of Calgary, Alberta, Canada. He holds a Canada Research Chair (CRC) in Mobile Multi-Sensors Geomatics Systems. El-Sheimy's area of expertise is in the integration of GPS/INS/imaging sensors for mapping and GIS applications with special emphasis on the use of

multi-sensors in mobile mapping systems. He achieved a B.Sc. (Honor) degree in civil engineering and an M.Sc. Degree in surveying engineering from Ain Shams University, Egypt, and a Ph.D. in geomatics engineering from the University of Calgary. Currently, El-Sheimy is the chair of the International Society for Photogrammetry and Remote Sensing Working Group on "Integrated Mobile Mapping Systems," the vice-chair of the special study group for mobile multi-sensor systems of the International Association of Geodesy, and the chairman of the International Federation of Surveyors (FIG) working group C5.3 on Integrated Positioning, Navigation and Mapping Systems. 

Inside GNSS